EurJOC
European Journal of Organic Chemistry

A Journal of
ChemPubSoc Europe

Accepted Article

Title: Mutual Kinetic Resolution of Racemic 3,4-Dihydro-3-methyl-2H-[1,4]benzoxazines with Acyl Chlorides of Racemic O-Phenyl Lactic Acids and DFT Modeling of Transition States

Authors: Marina Korolyova, Sergey Vakarov, Dmitry Kozhevnikov, Dmitry Gruzdev, Galina Levit, and Victor Krasnov

To be cited as: *Eur. J. Org. Chem.* 10.1002/ejoc.201800656

Link to VoR: http://dx.doi.org/10.1002/ejoc.201800656

Supported by
ACES Asian Chemical Editorial Society

WILEY-VCH

10.1002/ejoc.201800656

WILEY-VCH

Mutual Kinetic Resolution of Racemic 3,4-Dihydro-3-methyl-2*H*-[1,4]benzoxazines with Acyl Chlorides of Racemic *O*-Phenyl Lactic Acids and DFT Modelling of Transition States

Marina A. Korolyova,[a] Sergey A. Vakarov,[a] Dmitry N. Kozhevnikov,[a] Dmitry A. Gruzdev,[a] Galina L. Levit,[a] and Victor P. Krasnov*[a]

Abstract: The effect of electronic nature of the *para*-substituent in aromatic ring of 2-aryloxypropionyl chlorides on the stereochemical outcome of the acylation of 3,4-dihydro-3-methyl-2*H*-[1,4]benzoxazine and its 7,8-difluoro-containing analogue was studied. The geometry of diastereoisomeric transition states and the corresponding free Gibbs enthalpies of activation were determined using DFT calculations at the COSMO-CH_2Cl_2-B3LYP-D3-gCP/def2-TZVP (or def2-SVP)//B3LYP-D3-gCP/def2-SVP level of theory. It has been shown that a low-cost quantum chemical calculation at a chosen level of the theory describes well the quantitative dependence of the acylation selectivity on the reagents' structures. The obtained results indicate that the aromatic interactions between reagents play a significant role in the process of stereodifferentiation, ensuring high selectivity of the acylation of benzoxazines with 2-aryloxy acyl chlorides.

Introduction

The urgency of studying the mechanisms of stereoselective reactions is substantiated by the need for design of rational preparative approaches to enantiopure compounds. Kinetic resolution (KR) of racemates is one of the classical ways of obtaining individual enantiomers.[1] To determine the causes of stereoselectivity in the KR processes, quantum chemical calculations are used,[2] which make it possible to clarify the reaction mechanism and to determine the structure and energy of diastereoisomeric transition states. There are some examples of successful use of quantum chemical modelling to explain the reasons for stereoselectivity.[2a,3] At the same time, the achievement of a quantitative consistency between calculated and experimental data remains a difficult task.[3] To best of our knowledge, the only example of an accurate DFT-based simulation of the structure of a chiral catalyst for acylative KR of racemic secondary alcohols was described.[2a] Careful selection of the method of quantum chemical calculations and the level of theory, comparison of a wide range of calculated and experimental data allowed the authors to propose the structure of a highly selective catalyst for KR of racemic alcohols.

In recent years, we have studied the acylative KR[4] of racemic heterocyclic amines with enantiopure acyl chlorides, the derivatives of amino acids,[5] 2-arylpropionic[6] and 2-phenoxy acids.[7] One of the tasks that we aimed to solve in these studies was to establish the dependence of the stereochemical outcome of acylation on the reagents' structure and reaction conditions in order to improve the efficiency of KR.

[a] *Postovsky Institute of Organic Synthesis of RAS (Ural Branch), 22/20 S. Kovalevskoy/Akademicheskaya St., Ekaterinburg, 620990 Russia. E-mail: ca@ios.uran.ru*
Supporting information for this article is available on the WWW under http://dx.doi.org/10.1002/ejoc.…..

Recently we studied the stereoselective acylation of racemic 3-methylbenzoxazines **1a,b** (Figure 1) with racemic 2-phenoxy acyl chlorides.[7a] To determine the selectivity factor (*s*), which is the ratio of the rate constants of individual enantiomers ($s = k_{fast}/k_{slow}$),[8] we used the approach based on the interaction of racemic amines and racemic acylating agents, the so-called limiting variant of the mutual KR. This method allows accurate determination of the *s* value; in this case, the ratio and concentration of reagents and the reaction duration do not affect the stereochemical result of the process.[1,8] The selectivity factor in this case is equal to the ratio (*dr*) of diastereoisomeric amides formed during the acylation. We have found that the acylation of 3-methylbenzoxazines **1a,b** with 2-phenoxy acyl chlorides proceeds with high stereoselectivity (*s* up to 499).[7a] Based on the experimental data, we proposed a plausible model of diastereoisomeric transition states (TSs) arising during the reaction of 2-phenoxy acyl chlorides and amines.[7a] This model explained the observed stereoselectivity by a combined effect of electronic and steric factors.

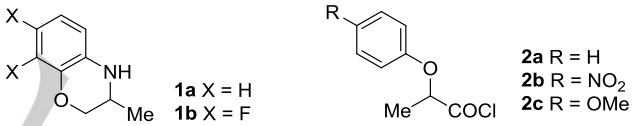

Figure 1. Structures of 3-methylbenzoxazines **1a,b** and 2-aryloxypropionyl chlorides **2a-c**.

The purpose of this work was to compare the stereoselectivity of acylation of racemic amines **1a,b** with 2-phenoxypropionyl chloride (**2a**) and its structural analogues bearing different *para*-substituents in the phenyl ring (2-(4-nitrophenoxy)propionyl chloride (**2b**) and 2-(4-methoxyphenoxy)propionyl chloride (**2c**)), to study the reaction mechanism, and to test the suitability of the quantum chemical modelling of diastereoisomeric transition states (TSs) by the DFT method in order to explain the observed selectivity.

Results and Discussion

Racemic 3-methylbenzoxazines **1a** and **1b** and individual (*S*)-enantiomers (*ee* ≥ 97%) were obtained as described previously.[5b, 9] The acylating agents **2a-c** were prepared starting from corresponding acids[10] upon treatment with an excess of oxalyl chloride (3 equiv.).

Acylation of racemic amines **1a** and **1b** was carried out in toluene or dichloromethane at +20 and −20 °C for 6 h; amine–acyl chloride molar ratio 2:1, initial amine concentration 0.1M

(Scheme 1). The reaction resulted in racemic (3*R**,2'*S**)- and (3*R**,2'*R**)-diastereoisomers of amides **3a-c** and **4a-c**. The diastereoisomeric ratio (*dr*) of amides **3a-c** and **4a-c** was determined by GC (each experiment was carried out in two parallel runs, see Supporting Information), which enabled us to calculate the selectivity factor *s* (Table 1). The major diastereoisomers (*R**,*S**)-**3-4a-c** were obtained in a diastereomerically pure form after recrystallization of the acylation products.

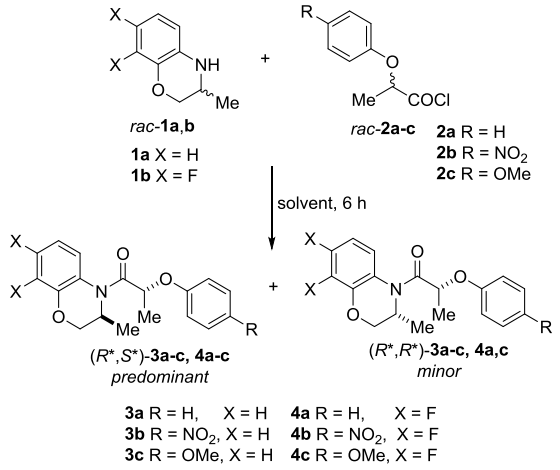

Scheme 1. Stereoselective acylation of amines **1a,b** with 2-aryloxypropionyl chlorides **2a-c**

For the correct assignment of the chromatographic peaks in GC, we synthesized mixtures of diastereomeric amides **3–4a-c** starting from racemic acyl chlorides **2a–c** and enantiopure benzoxazine (*S*)-**1a** or (*S*)-**1b** in stoichiometric amounts (in the presence of *N,N*-diethylaniline as an HCl acceptor); the ratio of (*S,S*)- and (*R,S*)-diastereomers was about 1:1 (for experimental details, see Supporting Information).

To assign the configuration in the resulting amides **3a-c** and **4a-c**, we carried out the acylation of enantiopure (*S*)-amines **1a** and **1b** with 2 equiv. of racemic 2-phenoxypropionyl chlorides **2a-c** in the presence of *N*,*N*-diethylaniline (as a HCl acceptor) (Scheme 2). As a result, diastereoisomerically enriched amides **3a-c** and **4a-c** and unreacted enantiomerically enriched acyl chlorides **2a-c** were formed. The latter were subjected to alkaline hydrolysis under mild conditions to afford corresponding acids **5a-c** (Scheme 2). Comparison of the sign of optical rotation of the isolated acids **5a-c** with the literature data[11] made it possible to conclude that they and, consequently, unreacted acyl chlorides **2a-c** were enriched with (*S*)-enantiomers. Thus, from these results it follows that in all cases (*S*)-amines **1a,b** react faster with (*R*)-enantiomers of acyl chlorides **2a-c**.

Table 1. Stereoselectivity in acylation of 3,4-dihydro-3-methyl-2*H*-[1,4]-benzoxazines **1a** and **1b** with racemic acyl chlorides **2a-c**

Amine	Acyl chloride	Solvent	Reaction temperature, °C	Selectivity factor *s*
1a	**2a** (R = H)	toluene	+20	35[7a]
1a	**2a** (R = H)	CH_2Cl_2	+20	17[7a]
1a	**2a** (R = H)	CH_2Cl_2	–20	25[7a]
1b	**2a** (R = H)	toluene	+20	56[7a]
1b	**2a** (R = H)	CH_2Cl_2	+20	17[7a]
1b	**2a** (R = H)	CH_2Cl_2	–20	62[7a]
1a	**2b** (R = NO_2)	toluene	+20	70
1a	**2b** (R = NO_2)	CH_2Cl_2	+20	49
1a	**2b** (R = NO_2)	CH_2Cl_2	–20	85
1b	**2b** (R = NO_2)	toluene	+20	49
1b	**2b** (R = NO_2)	CH_2Cl_2	+20	49
1b	**2b** (R = NO_2)	CH_2Cl_2	–20	80
1a	**2c** (R = OMe)	toluene	+20	25
1a	**2c** (R = OMe)	CH_2Cl_2	–20	20
1b	**2c** (R = OMe)	toluene	+20	43
1b	**2c** (R = OMe)	CH_2Cl_2	–20	41

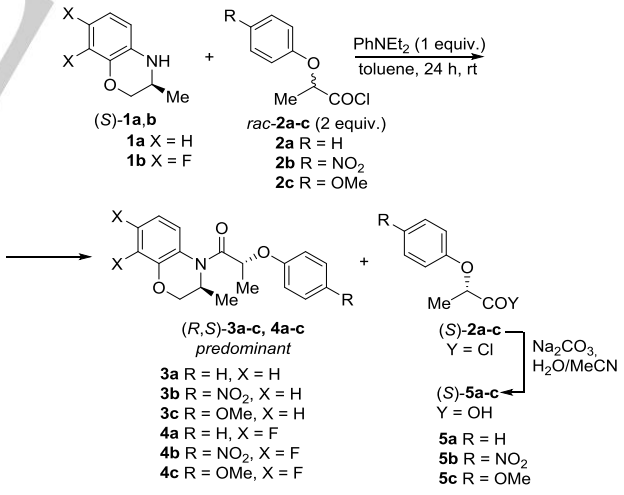

Scheme 2. KR of racemic acyl chlorides **2a-c** with (*S*)-3-methylbenzoxazines **1a,b**

As can be seen from Table 1, as a rule, the interaction of acyl chlorides **2a-c** with amines **1a, b** in toluene proceeded more selectively. Lowering the reaction temperature to −20 °C resulted in the expected increase in the selectivity factor *s*. For

example, when amine **1a** reacted with acyl chloride **2b** in dichloromethane at –20 °C, the selectivity factor *s* increased almost twice as compared with acylation at +20 °C (*cf.* *s* = 85 and *s* = 49). Comparison of the stereochemical results of acylation of 3-methylbenzoxazines **1a** and **1b** with 2-phenoxypropionyl chloride **2a** and acyl chlorides with electron-withdrawing (**2b**, R = NO_2) and electron-donating (**2c**, R = MeO) substituents in the aromatic ring allows to conclude that the electronic factors significantly affect the acylation stereoselectivity. Thus, among all studied acyl chlorides, 2-(4-nitrophenoxy)propionyl chloride (**2b**) demonstrated the highest selectivity in the acylation of amine **1a** in toluene at +20 °C (selectivity factor *s* = 70). In general, interaction of acyl chlorides **2a-c** with 7,8-difluorosubstituted amine **1b** in toluene proceeded with a relatively close stereoselectivity (selectivity factor *s* varied from 43 to 56). Interestingly, the acylation of 3-methylbenzoxazine **1b** with 2-(4-nitrophenoxy)propionyl chloride (**2b**) both in toluene and dichloromethane at +20 °C was equally selective (*s* = 49), while replacing toluene with dichloromethane when acyl chloride **2b** reacted with non-fluorinated amine **1a** resulted in a marked decrease in the selectivity factor *s* at the same temperature (70 *vs.* 49).

To simulate the stereoselectivity of acylation of 3,4-dihydro-3-methyl-2*H*-[1,4]benzoxazine (**1a**) and its 7,8-difluorosubstituted analogue **1b** with 2-aryloxy acyl chlorides **2a-c**, we performed DFT calculations of these reactions. Our task was to determine the mechanism of acylation and the causes of stereoselectivity, as well as to assess whether DFT method is suitable for quantitative estimation of stereoselectivity depending on the structure of reagents.

The classical concepts of acylation suppose a stepwise mechanism proceeding through the formation of a zwitterionic tetrahedral intermediate **Int** (Scheme 3, path *a*) or a S_N1-like mechanism involving the dissociation of the C–Cl bond at the first stage to form chloride-ion-stabilized cation **C+** (Scheme 3, path *b*).[12] At the same time, many studies of the kinetics of solvolysis and aminolysis of acyl chlorides, as well as the studies of other acyl transfer reactions, suggest a possible concerted mechanism involving the formation of uncharged TS in solvents of different types. In this case, the C–Cl bond is cleaved simultaneously with the formation of the C–nucleophile bond (transition state **TS** in Scheme 3, path *c*).[13] In some cases, conclusions about the concerted S_N2-like mechanism of the interaction of acyl chlorides with nucleophiles were made based on the experimental study of the reaction kinetics;[14] in other cases, they were confirmed by *ab initio* DFT calculations.[15] As has been shown by quantum chemical calculations, the realization of the concerted S_N2-like mechanism in the catalytic reaction of activated esters with amines[16] and catalytic *N*-acylation of lactams with symmetric anhydrides[3a] ensures the stereoselectivity of these reactions.

Obviously, there may be a competing pathway in the acylation reaction via an elimination–addition of the hydrogen atom at the chiral center of acyl chloride, which involves the formation of an achiral ketene intermediate. The most detailed investigation of racemization of a chiral acyl chloride was performed when studying the reaction of (*S*)-naproxen chloride [(*S*)-2-(6-methoxynaphth-2-yl)propionyl chloride] with different nucleophiles in the presence of various auxiliary bases.[17] It has been shown that complete or partial racemization of acyl chloride occurs when strong bases such as TEDA and DBU, as well as moderate bases (TEA) are used. It has been also supposed that in the presence of weak bases, the acylation proceeds via a direct substitution and no racemization is observed.[17]

In the case of acylation of racemic 3-methylbenzoxazines **1a** and **1b** with acyl chlorides **2a-c**, the reaction proceeded without any auxiliary base; we can consider amines **1a** and **1b** taken in excess as weak bases. Moreover, we have previously reported about preparation of enantiopure (*S*)-3,4-dihydro-3-methyl-2*H*-[1,4]benzothiazine (99.4% *ee*) via a KR protocol using enantiopure acyl chloride (*R*)-**2a** as a chiral resolving agent[7b] and clearly demonstrated that there was no racemization in the course of acylation. So, we excluded a ketene pathway when considering the acylation mechanisms.

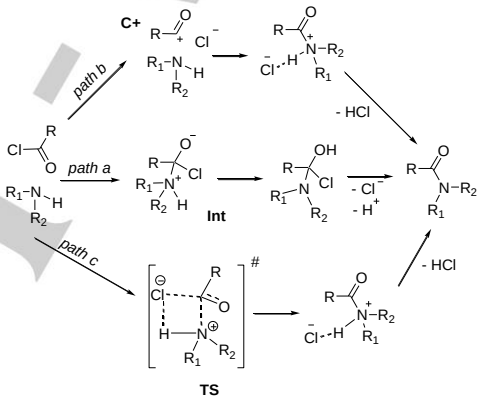

Scheme 3. Theoretically possible mechanisms of interaction of acyl chlorides with amines: path *a*, formation of the zwitterionic tetrahedral intermediate **Int**; path *b*, dissociation of the OC–Cl bond and formation of carbocation **C+** (S_N1-like); path *c*, the concerted mechanism of substitution at the carbonyl carbon atom (S_N2-like) resulting in transition state **TS**.

A preliminary calculation in the ORCA program using the Kohn–Sham density functional method at the B3LYP/TZVP level of theory with van der Waals correction of interactions between simple in structure aromatic and non-aromatic amines and acylating agents (see Supporting Information) showed the realization of S_N2-like mechanism with the formation of tetrahedral TS (see, for example, Figure 2).

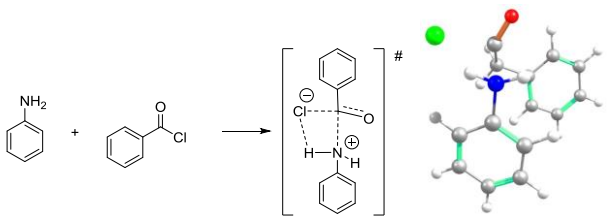

Figure 2. Transition state in the acylation of aniline with 2-phenylacetyl chloride by S_N2-like mechanism in dichloromethane (COSMO solvation model).

According to the calculation results, the length of N–CO bond in TSs depends on the amine nucleophilicity: in the reaction of acetyl chloride with ammonia, it is 2.149 Å; with aniline, 1.989 Å. In the reaction of 2-phenylacetyl chloride with aniline, the N–CO bond length is 1.984 Å; in the reaction of benzoyl chloride with ammonia, 2.089 Å. In this case, the Cl–CO bond length varies from 2.194 to 2.015 Å. The formation of a new C–N bond occurs with the simultaneous elimination of the HCl molecule. Such a concerted mechanism determines the TS geometry observed in all calculated reactions, in which the hydrogen and chlorine atoms are close to each other. The nucleophilic attack on the carbon atom of the carbonyl group is directed along the C=O bond at an angle of about 107° (*Bürgi–Dunitz trajectory*[18]). The interaction of lone pair of electrons located on the hybrid orbital of the *N* atom with the benzene ring of aniline determines the trajectory of approach of the amine to acyl chloride molecules: the benzene ring of aniline is oriented from the electron cloud of the carbonyl bond so that its *C*(1) atom is in the *trans*-conformation with the carbonyl *O* along the N–C bond formed. These factors determine the only possible position of the carbonyl group and the chlorine atom relative to the H–N bond in aniline in TS.

To determine the mechanism of the reaction between acyl chloride **2a** and amine **1a**, we performed scanning the total energy of the system (final single point energy E_{FSP}) in toluene at 298.15 K with a change in the length of the resulting C–N bond from 3.55 to 1.42 Å using the BLYP functional with TZVP basic set (see Supporting Information, Tables S2 and S3). A similar approach was used while determining the mechanism of hydrolysis of acyl chlorides.[19] We have found that the total energy of the system reaches a single maximum when the N–CO bond length is 1.65 Å, in the absence of energy minima in the range considered. This indicates the realization of the S_N2-like synchronous mechanism of acylation. In further calculations, we have assumed that the reaction of benzoxazine **1a** with acyl chloride **2a** proceeds via concerted S_N2-like mechanism.

Previously, we believed that the stereoselectivity of acylation of racemic 3-methylbenzoxazines **1a** and **1b** with 2-phenoxy acyl chlorides largely depends on the π-π interactions of the aromatic fragments of the reagents.[7a] But it is difficult to correctly take into account such noncovalent intermolecular interactions in DFT calculations.[20] It is known that, for example, global hybrid meta-GGA Minnesota functional MO62X,[21] global hybrid meta-GGA functional MPWIB95,[22] dispersion corrected GGA functional B97-D3,[23] and others are useful in the analysis of the energy of π-π interactions in different systems in the ground and excited states. These functionals require prolonged calculations. The Becke–Lee–Yang–Parr (B3LYP) functional has been often used as a low-cost test functional to compare the results obtained in it with calculations in more time-consuming functionals. However, in some cases, uncorrected B3LYP is unable to describe van der Waals complexes (π-π complexes) bound by medium-range interactions[24] and also overestimates the modulo value of energy of the ground state π-π interactions.[24, 25]

The use of dispersion corrected functionals (DFT-D) makes it possible to improve the accuracy of calculation. An approach of Prof. S. Grimme, i.e. the dispersion energy correction with the atom pairwise D3 method,[26] is one of the most successful methods. It is this approach that we used in our study. When using corrections such as the Becke–Johnson dispersion corrections D3 and geometrical counterpoise (gCP) correction of basis set superposition error, the B3LYP functional demonstrates good agreement between the results of calculations of aromatic π-π interactions, experimental data, and the results of benchmarking calculations,[25] and is one of the best for estimating noncovalent interactions.[27] Mean absolute deviations of π-π complexes formation energy in B3LYP-D3 functional benchmarking is about 1 kJ/mol.[28]

Acyl chlorides **2a-c** are conformationally mobile compounds, 3-methylbenzoxazines **1a** and **1b** have a conformational mobility of oxazine cycle, which substantially expands the conformational field and complicates the task for finding a TS structure. Therefore, the geometries of starting compounds, reagent complexes, and TSs formed during the interaction of 3-methylbenzoxazines **1a** and **1b** and 2-aryloxypropionyl chlorides **2a-c** were optimized by introduction of conformational requirements into the initial TS model structure. In addition to the eclipsed conformation of the leaving chlorine atom relative to the hydrogen atom of the amino group, we proceeded from the axial orientation of the methyl group at the chiral centre of benzoxazine, since the TS model structures with the equatorially oriented methyl group have a much higher energy than those with the axially oriented one. We also assume that the methyl group of benzoxazine in the *pseudo*-axial conformation is oriented in the opposite direction from the reaction centre, namely the carbonyl carbon atom, in both diastereomeric TSs.

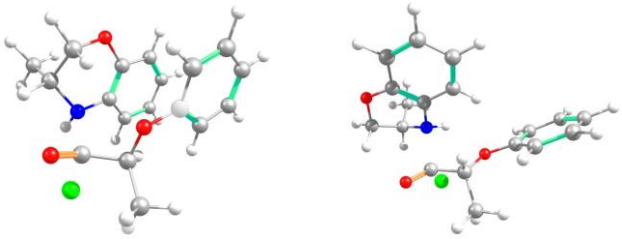

Figure 3. Structures of (3*R*,2'*S*)- (left) and (3*R*,2'*R*)- (right) diastereoisomeric TSs in the reaction of compounds **1a** and **2a** (calculated at the COSMO-CH_2Cl_2-B3LYP-D3-gCP/def2-TZVP//B3LYP-D3-gCP/def2-SVP level of theory).

When modelling the initial diastereomeric TS structures for the DFT optimization, arrangement of the benzene rings in reagents was given almost coplanar. At the first stage, geometric optimization and calculation of the Hessian were carried out in a vacuum at the B3LYP-D3-gCP/def2-SVP level of theory (all Cartesian coordinates and calculated energies are given in Supporting Information). As a result of subsequent geometric optimization in dichloromethane at the COSMO-CH_2Cl_2-B3LYP-

D3-gCP level of theory with both def2-SVP and def2-TZVP Ahlrichs basis sets, the coplanar arrangement of aromatic systems in (3*S*,2'*R*)-diastereoisomer of TS in the reaction of amine **1a** with acyl chloride **2a** was preserved (Figure 3, left; see also Supporting Information); the distance between the planes of benzene rings is 3.45–3.55 Å, which is typical for π-π interactions. The benzene rings in (3*R*,2'*R*)-diastereomeric TS take an almost orthogonal arrangement (Figure 3, right). Interestingly, the methyl group at the chiral centre of acyl chloride, as probably the largest substituent, is in the *trans*-conformation with respect to the nitrogen atom of benzoxazine, which agrees with the Felkin–Ahn rule.[29]

Apparently, the π-stacking with the parallel and shifted arrangement of the benzene rings of reagents takes place in the (3*S*,2'*R*)-TS and stabilizes it, decreasing the activation energy in comparison with (3*R*,2'*R*)-TS, in which we did not observe such π-stacking. It should be noted that the calculated structures of (3*R*,2'*R*)-TS with the abovementioned π-π interaction (calculation of the Hessian without preliminary geometric optimization) have a much larger free Gibbs activation energy (more than 50 kJ/mol) than the optimized ones, so we did not considered them. The diastereomeric TSs found for other 'amine–acyl chloride' pairs had the same structure as for **1a–2a** pair.

The values of activation energy in the reaction of acyl chlorides **2a-c** and amines **1a** and **1b**, which were calculated as the difference between the Gibbs energy of TS and reagents complex ($\Delta G^{\#}$) at –20 °C in dichloromethane (see Supporting Information) are presented in Table 2. The geometry of the reagents complexes is optimized "from the TS structure" by introducing a restriction, namely the Cl–C(O) bond length of 1.82 Å (as it is in the starting acyl chloride). In all cases, the zwitterionic tetrahedral intermediate **Int** (Scheme 3) was not found. The reagents complex corresponding to an energy minimum could claim a role of such an intermediate. However, the distance between the nitrogen atom of amine and the carbon atom of carbonyl group in acyl chloride in the complex is too large (3.09–4.19 Å) to form the C–N bond. The results obtained support the assumption that the acylation of benzoxazines **1a** and **1b** with 2-aryloxy acyl chlorides **2a-c** proceeds through the tetrahedral transition state, which is at the energy maximum in the reaction pathway, which corresponds to a synchronous S_N2-like mechanism.

A comparison of the experimentally observed stereoselectivity with the calculated difference of activation energies for diastereomeric TSs was performed. In the reaction of 2-phenoxypropionyl chloride (**2a**) with (*R*)-3-methylbenzoxazine **1a**, the calculated (def2-TZVP) activation energy of the (3*R*,2'*R*)-TS formation is higher than that of (3*S*,2'*R*)-TS by 6.63 kJ/mol (selectivity factor s_{calc} = 21 was derived from calculated $\Delta\Delta G^{\#}$), which agrees well with the observed stereoselectivity (s_{exp} = 25) corresponding to $\Delta\Delta G^{\#}$ 6.77 kJ/mol. The highest calculated $\Delta\Delta G^{\#}$ value (regardless of the basis used) for reactions of amine **1a** was obtained in the reaction with acyl chloride **2b**; the lowest, in the reaction of the same amine with acyl chloride **2c**. Such a change in the stereoselectivity of reactions of amine **1a** as a function of the *para*-substituent structure is consistent with the experimental data. In computations of the amine **1b** reactions (in the def2-TZVP basis set), the maximum $\Delta\Delta G^{\#}$ value was obtained in the reaction with acyl chloride **2b**; minimum, in the reaction with compound **2a**. The experimental stereoselectivity of the reactions of amine **1b** with acyl chlorides increased in the series: **2c** < **2a** < **2b**. The discrepancy between the calculated stereoselectivity and the experimental data can be related to the realization of the interactions N-H…OPh in (3*R*,2'*R*)-TS. According to the computation results, the distance between the hydrogen atom of the amino group of benzoxazine and the oxygen of 2-aryloxy group in (3*R*,2'*R*)-TS varied from 1.96 to 2.49 Å, depending on the structure of the reagents, which does not exclude the Coulomb interaction or less likely the hydrogen bonding. Therefore, in (3*R*,2'*R*)-TS, the oxygen atom of 2-aryloxy group can compete for the proton of the NH group with the leaving chlorine atom. In this case, we did not found similar interactions in (3*S*,2'*R*)-TS. Their realization contributes to the stabilization of (3*R*,2'*R*)-TS, significantly lowering its energy relative to the energy of (3*S*,2'*R*)-TS, which leads to a decrease in the calculated stereoselectivity. Probably, in the case of the reaction of benzoxazine **1b** and acyl chloride **2b**, the contribution of the N-H…OPh polar interactions to a decrease in the calculated energy of (3*R*,2'*R*)-TS is proved to be overestimated within the framework of the model studied, and reduces the calculated selectivity factor *s* in comparison with the experimental result.

Table 2. Calculated activation energies ($\Delta G^{\#}$) in the reactions of (*R*)-benzoxazines **1a** and **1b** with acyl chlorides **2a-c** at –20 °C in CH_2Cl_2

Basis	Acyl chloride–amine	$\Delta G^{\#}$, kJ/mol	$\Delta\Delta G^{\#}$, kJ/mol	
			Calculated	Experimental[a]
def2-SVP	(*R*)-**1a**–(*S*)-**2a** (*R*)-**1a**–(*R*)-**2a**	41.53 46.81	5.28	6.77
def2-TZVP	(*R*)-**1a**–(*S*)-**2a** (*R*)-**1a**–(*R*)-**2a**	28.19 34.82	6.63	
def2-SVP	(*R*)-**1b**–(*S*)-**2a** (*R*)-**1b**–(*R*)-**2a**	47.70 56.66	8.96	8.68
def2-TZVP	(*R*)-**1b**–(*S*)-**2a** (*R*)-**1b**–(*R*)-**2a**	38.66 45.45	6.79	
def2-SVP	(*R*)-**1a**–(*S*)-**2b** (*R*)-**1a**–(*R*)-**2b**	42.61 54.93[b]	12.32	9.34
def2-TZVP	(*R*)-**1a**–(*S*)-**2b** (*R*)-**1a**–(*R*)-**2b**	32.73 41.54[b]	8.81	
def2-TZVP	(*R*)-**1b**–(*S*)-**2b** (*R*)-**1b**–(*R*)-**2b**	45.79 55.00[b]	9.21	9.21
def2-SVP	(*R*)-**1a**–(*S*)-**2c** (*R*)-**1a**–(*R*)-**2c**	42.46 47.55	5.09	6.29
def2-TZVP	(*R*)-**1a**–(*S*)-**2c** (*R*)-**1a**–(*R*)-**2c**	29.91 35.87	5.96	
def2-TZVP	(*R*)-**1b**–(*S*)-**2c** (*R*)-**1b**–(*R*)-**2c**	39.38 46.63[b]	7.25	7.81

[a] Experimental $\Delta\Delta G^{\#}$ was derived from the selectivity factor *s* according to the

equation: $s = k_{RS} / k_{RR} = e^{-(\Delta G\#_{RS} - \Delta G\#_{RR}) / RT}$ (see, for example [3b]).

[b] Geometric optimization of the reagents complex was performed from the model TS structure.

The *para*-substituent in the benzene ring of acyl chloride affects the charge of the oxygen atom of 2-aryloxy group, so it can be assumed that in the presence of an electron-withdrawing substituent (acyl chloride **2b**, R = NO_2) in this position, the absolute value of the partially negative charge on the oxygen atom of the 2-aryloxy group is decreased and its competition with the chlorine atom for the leaving hydrogen of the amino group of benzoxazine is weakened. The latter leads to a decrease in the probability of formation of (3*R*,2'*R*)-TS with strong Coulomb PhO…H-N interaction and thereby increases the stereoselectivity of acylation of amine **1a** with acyl chloride **2b** chloride as compared with selectivity of the reaction of the same amine with unsubstituted reagent **2a** (R = H).

In general, the calculated difference in activation energies for diastereomeric TSs increases with the electron-withdrawing properties of the *para*-substituent in the benzene ring of acyl chloride, which corresponds to the observed experimental pattern.

It should be noted that the low-cost B3LYP-D3-gCP hybrid functional proved very well in quantifying the stereoselectivity of acylation. When using the triple-ζ def2-TZVP basis set, the error in determining $\Delta\Delta G^{\#}$ did not exceed 2 kJ/mol, and, in general, the dependence of stereoselectivity on the amine and acylating agent structures is described correctly at this level of theory. Complication of the basic set in the transition from def2-SVP to def2-TZVP leads to a decrease in the absolute values of the activation energies for both diastereomers.

In general, the length of the formed N–C(O) bond is larger in (3'*S*,2'*R*)-TS than in (3*R*,2'*R*)-TS for all 'amine–acyl chloride' pairs. The length of the breaking C–Cl bond in TSs calculated using both def2-SVP and def2-TZVP basis sets depends on the amine structure (see Supporting Information). Thus, in the reaction of 2-phenoxypropionyl chloride **2a** with benzoxazine **1a**, it is shorter than in the reaction of reagent **2a** with difluorobenzoxazine **1b**. On the other hand, when computation was performed in the def2-TZVP basis set, the N–CO bond in the transition from amine **1a** to amine **1b** decreased in both diastereomeric TSs. Perhaps, the revealed dependence indicates the need for a closer contact of the nitrogen atom of the weak nucleophile **1b** with the carbonyl carbon atom of acyl chloride for realization of acylation. The shortening of the N–CO bond leads to an increase in stereodiscrimination, which is manifested by an increase in the experimental value of the selectivity factor *s* of acylation of amine **1a** with acyl chloride **2a** compared with that of its 7,8-difluoro-containing analogue **1b**.

The geometry of the reagents complex when calculating using both basis sets depends on the initial structure subjected to optimization. Thus, in the (3*R*,2'*R*)-complex of reagents **1a** and **2b** found from the DFT-optimized TS structure (see Supporting Information), the practically orthogonal arrangement of the aromatic systems is preserved, as in the TS shown in Figure 4 (left); however, in this case, the calculated value of $\Delta\Delta G^{\#}$ (not shown in Table 2) does not correspond to the experimental selectivity factor *s*. At the same time, optimization of the geometry of (3*R*,2'*R*)-complex from the initial model TS structure with almost coplanar arrangement of the benzene rings in reagents (see Supporting Information) leads to the reagents complex shown in Figure 4 (right), and a much more accurate values of the activation energy and the selectivity factor *s*.

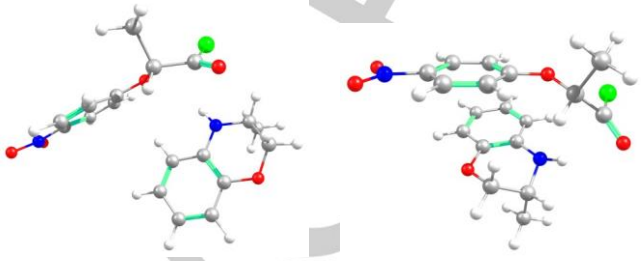

Figure 4. Structures of (3*R*,2'*R*)-complex of reagents **1a** and **2b** (calculated at the COSMO-CH_2Cl_2-B3LYP-D3-gCP/def2-TZVP//B3LYP-D3-gCP/def2-SVP level of theory from the optimized TS (left) and starting model geometry of TS with coplanar arrangement of benzene rings (right)).

As can be seen from Table 2, the computations at the COSMO-CH_2Cl_2-B3LYP-D3-gCP/def2-TZVP//B3LYP-D3-gCP/def2-SVP levels of theory are consistent with the experimental values of the selectivity factor in the acylation of benzoxazines **1a** and **1b** with acyl chlorides **2a-c**. It can be concluded that the proposed concerted four-center mechanism of acylation and the stereodifferentiation model, which is based on aromatic interactions in (3*S*,2'*R*)-TS and the absence of those in (3*R*,2'*R*)-TS, describe well the experimental observations on the effect of the amine and acylating reagent structures on the efficiency of acylative KR.

Probably, π-stacking takes place in the reagents complexes of both (3*S*,2'*R*)- and (3*R*,2'*R*)-configuration (at least in pairs of reagents **1a**-**2b**, **1b**-**2b**, **1a-2c** and **1b**-**2c**; see Cartesian coordinates and Figures in Supporting Information). However, in the case of (3*S*,2'*R*)-diastereomers, it plays a role in the stabilization of TS; in the case of (3*R*,2'*R*)-diastereomers, it increases the activation barrier during the formation of TS. An increase in the calculated parameter $\Delta\Delta G^{\#}$ of the reaction of benzoxazines **1a** and **1b** with 4-nitrophenoxy-substituted reagent **2b** in comparison with acyl chloride **2a** is likely to be due to stronger aromatic interactions. π-Stacking between the electron-withdrawing ring of reagent **2b** and the electron-donating aromatic cycle of benzoxazine in (3*S*,2'*R*)-TS is realized both by the Coulomb forces and by the London dispersion forces. On the contrary, the presence of methoxy group in position 4 of the aromatic ring of acyl chloride weakens the π-π interactions in (3*S*,2'*R*)-TS and reagents **1a-2c** complexes as compared with **1a-2b** complexes, which leads to a decrease in selectivity while transition from acylating agent **2b** (R = NO_2) to **2c** (R = OMe). At the same time, as shown in the computation of the reactions of benzoxazines **1a** and **1b** with acyl chloride **2c**, sandwich π-stacking probably takes place in both (3*R*,2'*R*)- and (3*S*,2'*R*)-complexes of reagents. However, based on a comparison of the experimental and calculated values of $\Delta\Delta G^{\#}$ for the reactions of acylating agent **2a** (R = H) it

can be asserted that there is no sandwich π-stacking in the (3*R*,2'*R*)-complexes of amines **1a** and **1b** with acyl chloride **2a**.

In general, we can conclude that the stereoselectivity in KR is determined by how π-stacking of aromatic fragments reduces the total electronic energy of reagents complexes and transition states. For the reagents **1b-2b**, the selectivity factor *s* is the maximum in the whole series of reactions, possibly because π-stacking significantly reduces the energy of (3*R*,2'*R*)-diastereomeric complex and increases the relative activation energy of the formation of (3*R*,2'*R*)-amide. In pairs of reagents **1a-2c** and **1b-2c**, π-stacking also occurs in the (3*R*,2'*R*)-complexes, but it appears to be weaker than in the (3*R*,2'*R*)-complexes with acyl chloride **2b**, and reduces the energy of the reagents complexes to a much lesser degree and, accordingly, less contributes to a relative increase in the activation energy of the (3*R*,2'*R*)-amide formation.

A comparison of the experimental data and the results of DFT modelling has shown that the stereoselectivity of KR is determined by aromatic interactions in the diastereomeric transition states and reagent complexes that are stronger in (3*S*,2'*R*)- than in (3*R*,2'*R*)-diastereomeric TSs, which results in the preferred formation of (3*S*,2'*R*)-amides. The low-cost computation by means of the corrected B3LYP-D3-gCP functional can be considered very suitable for modelling the TS structures arising during the acylation of benzoxazines **1a, b** by acyl chlorides **2a-c**.

Conclusions

Thus, we studied the stereoselective acylation of racemic 3,4-dihydro-3-methyl-2*H*-[1,4]benzoxazine and its 7,8-difluoro-substituted analog with 2-phenyloxypropionyl chlorides. We have found that the stereoselectivity of acylation of 3-methyl-benzoxazines with 2-aryloxy acyl chlorides is largely determined by the electronic structure of the reagents. DFT calculations of the free Gibbs energies of diastereomeric transition states and reagents complexes arising during the acylation of benzoxazines with 2-aryloxy acyl chlorides were carried out; the geometry of TSs was optimized at the COSMO-CH_2Cl_2-B3LYP-D3-gCP/def2-TZVP (or def2-SVP)//B3LYP-D3-gCP/def2-SVP levels of theory, the corresponding activation energies were found. It has been demonstrated that in all cases the acylation proceeds by the concerted S_N2-like mechanism. When this mechanism is realized, (3*S*,2'*R*)-diastereomeric TSs are stabilized by π-π interactions of the aromatic fragments of the reagents; such interactions are absent in (3*R*,2'*R*)-diastereomeric TSs. This determines the predominant formation of (3*S*,2'*R*)-amides as acylation products. The stereochemical outcome of KR is largely dependent on the structure of the diastereomeric TSs and the corresponding reagent complexes. In the diastereomeric TSs, the interaction of the hydrogen atom of NH group and the leaving chlorine takes place by the hydrogen bonding. In the case of (3*R*,2'*R*)-diastereomeric TSs, its stabilization also occurs due to the polar interaction of the hydrogen atom of the amine NH group with the oxygen atom of the 2-phenoxy group of acyl chloride. The proposed mechanism of stereoselective acylation describes well the experimentally observed effect of the substituent in position 4 of the aromatic cycle of acyl chloride on the selectivity factor *s*. A good correlation of the calculated (corrected functional B3LYP-D3-gCP) and experimental data was achieved for the reactions of benzoxazines differing in nucleophilicity with different acyl chlorides. This result allows us to conclude that the chosen low-cost level of theory is suitable for describing the quantitative dependence of the selectivity factor *s* on the reagents structure in the series of reactions studied. So, the method makes it possible to successfully take into account noncovalent intermolecular interactions both in TSs and in the reagent complexes.

Experimental Section

General Methods: All reactions were carried out under an argon atmosphere in dried glassware unless otherwise noted. The ^{1}H, ^{13}C and ^{19}F NMR spectra were recorded on Bruker DRX-400 (400, 100 and 376 MHz, respectively) or Bruker Avance 500 (500, 126 and 470 MHz, respectively) spectrometers with TMS and hexafluorobenzene as the internal standards. The NMR spectra of amides **3b**,**c** and **4b**,**c** were recorded in DMSO-d_6 at 100 °C, the NMR spectra of other compounds, in $CDCl_3$ at ambient temperature. Melting points were obtained on a SMP3 apparatus (Barloworld Scientific, UK) and are uncorrected. Elemental analysis was performed using a Perkin Elmer 2400 II analyzer. Analytical TLC was performed using Sorbfil plates (Imid, Russia). Flash column chromatography was performed using Silica gel (230–400 mesh) (Alfa Aesar, UK). The HMRS of acid (*S*)-**5c** was obtained on a Bruker maXis Impact HD mass spectrometer (ESI). Analytical HPLC of acids **5a-c** was performed on a Knauer Smartline-1100 instrument using Chiralpak AD (**5a** and **5c**) and Chiralcel OD-H (**5b**) columns (250 × 4.6 mm; Daicel, Japan); detection at 220 nm, 1 mL/min flow rate, *n*-hexane–*i*-PrOH–CF_3COOH 20:1:0.02: $\tau_{(R)\text{-}\mathbf{5a}}$ 9.3 min, $\tau_{(S)\text{-}\mathbf{5a}}$ 7.3 min, $\tau_{(R)\text{-}\mathbf{5b}}$ 23.4 min, $\tau_{(S)\text{-}\mathbf{5b}}$ 20.5 min, $\tau_{(S)\text{-}\mathbf{5c}}$ 12.3 min, $\tau_{(R)\text{-}\mathbf{5c}}$ 15.4 min. Optical rotations were measured on a Perkin Elmer M341 polarimeter. GC analyses of amides **3a-c** and **4a-c** was performed using a Shimadzu GC-2010 instrument with a ZB-5 capillary column (30 m × 0.25 mm × 0.25 μm). Racemic 3,4-dihydro-3-methyl-2*H*-[1,4]benzoxazine (**1a**) and 7,8-difluoro-3,4-dihydro-3-methyl-2*H*-[1,4]benzoxazine (**1b**),[9a] and their (*S*)-enantiomers (*S*)-**1a** and (*S*)-**1b**),[5b,9bc] racemic acids **5a**,[10b] **5b**,[10c] and **5c**[10a] were obtained according to the reported procedures. Acyl chloride **2a**, amides (R^*,S^*)-**3a** and (R^*,S^*)-**4a** were described earlier.[7a]

Acyl Chlorides 2a-c. General Procedure: Oxalyl chloride (1.31 mL, 15 mmol) and DMF (5 μL) were added to a solution of the appropriate 2-phenoxycarbonyl acid (5 mmol) in CH_2Cl_2 (20 mL) under stirring at room temperature. The reaction mixture was stirred for 6 h at room temperature and evaporated to dryness under reduced pressure. The residue was dried over P_2O_5 in vacuo. Acyl chlorides **2a-c** are unstable during storage, so they were used freshly prepared (chemical purity of at least 97% according to ^{1}H NMR spectroscopy).

(*RS*)-2-(4-Nitrophenoxy)propionyl Chloride (2b): Yield 1.14 g (99%), yellowish oil. ^{1}H NMR (500 MHz, $CDCl_3$): δ = 8.22-8.25 (m, 2 H, Ar), 6.94-6.97 (m, 2 H, Ar), 5.06 (q, *J* = 6.8 Hz, 1 H, C^2H), 1.82 (d, *J* = 6.8 Hz, 3 H, Me) ppm.

(*RS*)-2-(4-Methoxyphenoxy)propionyl Chloride (2c): Yield 1.06 g (99%), yellowish oil. ^{1}H NMR (400 MHz, $CDCl_3$): δ = 6.84 (app. s, 4 H, Ar), 4.86 (q, *J* = 6.8 Hz, 1 H, C^2H), 3.76 (s, 3 H, OMe), 1.72 (d, *J* = 6.8 Hz, 3 H, Me) ppm.

Acylation of Racemic Amines 1a and 1b with Racemic Acyl Chlorides 2a-c. General Procedure: A solution of the appropriate acyl chloride **2a**, **2b**, or **2c** (0.5 mmol) in the appropriate solvent (5 mL) was added to a solution of amine **1a** or **1b** (1 mmol) in the same solvent (5 mL) at +20 or –20 °C. The reaction mixture was kept in a thermostat at a given temperature for 6 h; then successively washed with 4 M HCl (2 × 4 mL), saturated aqueous NaCl (4 × 5 mL), 5% $NaHCO_3$ (2 × 5 mL), and water (2 × 5 mL). The organic layer was separated, dried over Na_2SO_4, and evaporated under reduced pressure. The residue was analyzed by GC (Shimadzu GC-2010), then recrystallized to yield the major (*R**,*S**)-diastereomers of amides **3a-c** and **4a-c**.

(*R,*S**)-3,4-Dihydro-3-methyl-*N*-(2-(4-nitrophenoxy)propionyl)-2*H*-[1,4]benzoxazine ((*R**,*S**)-3b)**: Yield 104 mg (61%), white solid, m.p. 129-130 °C (*n*-hexane-EtOAc). GC: $\tau_{(R,S)\text{-}\mathbf{3b}}$ = 32.4 min, $\tau_{(R,R)\text{-}\mathbf{3b}}$ = 33.4 min, (*R**,*S**)-(*R**,*R**) 99.7:0.3. ^{1}H NMR (500 MHz, DMSO-d_6, 100 °C): δ = 8.13 (app. d, *J* = 9.2 Hz, 2 H, Ar acyl), 7.65-7.67 (m, 1 H, C^5H benzoxazine), 6.99-7.06 (m, 3 H, C^7H benzoxazine and Ar acyl), 6.88 (dd, *J* = 8.2, 1.1 Hz, 1 H, C^8H benzoxazine), 6.83-6.86 (m, 1 H, C^6H benzoxazine), 5.62 (q, *J* = 6.3 Hz, 1 H, C^2H acyl), 4.61-4.66 (m, 1 H, C^3H benzoxazine), 4.20 (dd, *J* = 11.0, 1.5 Hz, 1 H, C^2H_A benzoxazine), 4.08 (dd, *J* = 11.0, 2.7 Hz, 1 H, C^2H_B benzoxazine), 1.60 (d, *J* = 6.3 Hz, 3 H, Me acyl), 1.16 (d, *J* = 6.7 Hz, 3 H, Me benzoxazine) ppm. ^{13}C NMR (125 MHz, DMSO-d_6, 100 °C): δ = 167.21, 161.56, 145.65, 141.21, 125.35, 125.10, 124.16, 122.68, 119.63, 115.95, 115.09, 71.58, 69.07, 45.13, 16.51, 14.82 ppm. Anal. calcd. for $C_{18}H_{18}N_2O_5$: C, 63.15; H, 5.30; N, 8.18. Found: C, 63.04; H, 5.26; N, 8.06.

(*R,*S**)-7,8-Difluoro-3,4-dihydro-3-methyl-*N*-(2-(4-nitrophenoxy)-propionyl)-2*H*-[1,4]benzoxazine ((*R**,*S**)-4b)**: Yield 127 mg (67%), white solid, m.p. 183-184 °C (*n*-hexane-EtOAc). GC: $\tau_{(R,S)\text{-}\mathbf{4b}}$ = 32.9 min, $\tau_{(R,R)\text{-}\mathbf{4b}}$ = 33.9 min, (*R**,*S**)-(*R**,*R**) 98.4:1.6. ^{1}H NMR (500 MHz, DMSO-d_6, 100 °C): δ = 8.13-8.20 (m, 2 H, Ar acyl), 7.55 (ddd, *J* = 9.3, 5.5, 2.6 Hz, 1 H, C^5H benzoxazine), 7.02-7.08 (m, 2 H, Ar acyl), 6.83 (app. dt, *J* = 9.8, 8.2 Hz, 1 H, C^6H benzoxazine), 5.64 (q, *J* = 6.3 Hz, 1 H, C^2H acyl), 4.66 (qdd, *J* = 6.8, 2.7, 1.5 Hz, 1 H, C^3H benzoxazine), 4.37 (dd, *J* = 11.1, 1.5 Hz, 1 H, C^2H_A benzoxazine), 4.17 (dd, *J* = 11.1, 2.9 Hz, 1 H, C^2H_B benzoxazine), 1.58 (d, *J* = 6.4 Hz, 3 H, Me acyl), 1.18 (d, *J* = 6.8 Hz, 3 H, Me benzoxazine) ppm. ^{13}C NMR (125 MHz, DMSO-d_6, 100 °C): δ = 167.41, 161.41, 146.74 (dd, *J* =243.0, 10.1 Hz), 141.28, 138.63 (dd, *J* = 242.8, 17.3 Hz), 136.04 (dd, *J* = 10.2, 3.4 Hz), 125.15, 120.65, 118.85 (dd, *J* = 8.0, 4.3 Hz), 115.14, 106.49 (d, *J* = 18.3 Hz), 71.63, 69.59, 45.18, 16.24, 14.72 ppm. ^{19}F NMR (470 MHz, DMSO-d_6, 100 °C): δ = 21.27-21.41 (m, 1 F, C^7F), 2.31 (ddd, *J* = 20.9, 8.0, 1.6 Hz, 1 F, C^8F) ppm. Anal. calcd. for $C_{18}H_{16}F_2N_2O_5$: C, 57.15; H, 4.26; N, 7.40; F, 10.04. Found: C, 56.94; H, 4.08; N, 7.30; F 9.77.

(*R,*S**)-3,4-Dihydro-3-methyl-*N*-(2-(4-methoxyphenoxy)propionyl)-2*H*-[1,4]benzoxazine ((*R**,*S**)-3c)**: Yield 106 mg (65%), white solid, m.p. 87-89 °C (*n*-hexane-EtOAc). GC: $\tau_{(R,S)\text{-}\mathbf{3c}}$ = 29.1 min, $\tau_{(R,R)\text{-}\mathbf{3c}}$ = 29.8 min, (*R**,*S**)-(*R**,*R**) 99.3:0.7. ^{1}H NMR (500 MHz, DMSO-d_6, 100 °C): δ = 7.63 (app. d, *J* = 7.9 Hz, 2 H, C^5H benzoxazine), 7.05 (ddd, *J* = 8.2, 7.2, 1.3 Hz, 1 H, C^7H benzoxazine), 6.85-6.89 (m, 2 H, Ar acyl), 6.74-6.81 (m, 4 H, C^6H, C^8H benzoxazine and Ar acyl), 5.27 (q, *J* = 6.4 Hz, 1 H, C^2H acyl), 4.67 (qdd, *J* = 6.8, 2.5, 1.6 Hz, 1 H, C^3H benzoxazine), 4.16 (dd, *J* = 11.0, 1.6 Hz, 1 H, C^2H_A benzoxazine), 3.96 (dd, *J* = 11.0, 2.7 Hz, 1 H, C^2H_B benzoxazine), 3.68 (s, 3 H, OMe), 1.51 (d, *J* = 6.4 Hz, 3 H, Me acyl), 1.11 (d, *J* = 6.8 Hz, 3 H, Me benzoxazine) ppm. ^{13}C NMR (125 MHz, DMSO-d_6, 100 °C): δ = 168.43, 153.86, 150.36, 145.58, 125.12, 124.24, 122.87, 119.51, 116.40, 115.87, 114.42, 71.67, 69.07, 55.10, 44.80, 16.77, 14.74 ppm. Anal. calcd. for $C_{19}H_{21}NO_4$: C, 69.71; H, 6.47; N, 4.28. Found: C, 69.74; H, 6.30; N, 4.13.

(*R,*S**)-7,8-Difluoro-3,4-dihydro-3-methyl-*N*-(2-(4-methoxyphenoxy)-propionyl)-2*H*-[1,4]benzoxazine ((*R**,*S**)-4c)**: Yield 109 mg (60%), white solid, m.p. 105-107 °C (*n*-hexane-EtOAc). GC: $\tau_{(R,S)\text{-}\mathbf{4c}}$ = 29.1 min, $\tau_{(R,R)\text{-}\mathbf{4c}}$ = 29.8 min, (*R**,*S**)-(*R**,*R**) 99.5:0.5. ^{1}H NMR (500 MHz, DMSO-d_6, 100 °C): δ = 7.53 (ddd, *J* = 9.3, 5.5, 2.5 Hz, 1 H, C^5H benzoxazine), 6.78-6.87 (m, 5 H, Ar acyl and C^6H benzoxazine), 5.29 (q, *J* = 6.3 Hz, 1 H, C^2H acyl), 4.71 (qdd, *J* = 6.8, 2.6, 1.4 Hz, 1 H, C^3H benzoxazine), 4.33 (dd, *J* = 11.0, 1.4 Hz, 1 H, C^2H_A benzoxazine), 4.06 (dd, *J* = 11.0, 2.6 Hz, 1 H, C^2H_B benzoxazine), 3.69 (s, 3 H, OMe), 1.49 (d, *J* = 6.3 Hz, 3 H, Me acyl), 1.13 (d, *J* = 6.8 Hz, 3 H, Me benzoxazine) ppm. ^{13}C NMR (125 MHz, DMSO-d_6, 100 °C): δ = 168.61, 153.96, 150.21, 146.63 (dd, *J* =242.5, 9.9 Hz), 138.61 (dd, *J* = 244.4, 15.3 Hz), 135.94 (dd, *J* = 10.0, 3.2 Hz), 120.83, 118.88 (dd, *J* = 8.0, 4.3 Hz), 116.43, 114.45, 106.37 (d, *J* = 18.3 Hz), 71.79, 69.62, 55.10, 45.91, 16.46, 14.63 ppm. ^{19}F NMR (470 MHz, DMSO-d_6, 100 °C): δ = 20.95-21.13 (m, 1 F, C^7F), 2.11 (ddd, *J* = 21.0, 7.9, 2.0 Hz, 1 F, C^8F) ppm. Anal. calcd. for $C_{19}H_{19}F_2NO_4$: C, 62.81; H, 5.27; N, 3.85; F, 10.46. Found: C, 63.04; H, 5.17; N, 3.90; F 10.44.

Kinetic Resolution of Racemic Acyl Chlorides 2a–c with (*S*)-Amines 1a,b. General Procedure: A solution of the appropriate acyl chloride (0.6 mmol) in toluene (2 mL) was added to a solution of (*S*)-amine **1a** or **1b** (0.3 mmol) and $PhNEt_2$ (44.8 mg, 0.3 mmol) in toluene (4 mL) at +20 °C. The reaction mixture was kept in a thermostat at +20 °C for 24 h and then evaporated to dryness under reduced pressure. The residue was dissolved in MeCN (10 mL), then saturated aqueous Na_2CO_3 (10 mL) was added. The reaction mixture was stirred for 1 h, after which MeCN was removed by evaporation under reduced pressure. An aqueous solution was extracted with $CHCl_3$ (2 × 5 mL). The organic layers were washed with 4 M HCl (2 × 4 mL), saturated aqueous NaCl (4 × 5 mL), and water (2 × 5 mL). The organic layer was separated, dried over Na_2SO_4, and evaporated under reduced pressure. The residue was analyzed by GC.

Alkaline aqueous solutions (after extraction with $CHCl_3$) were combined, acidified with 4 M HCl to pH 1–2, and extracted with $CHCl_3$ (2 × 5 mL). The organic layer was separated, washed with saturated aqueous NaCl (2 × 5 mL), dried over Na_2SO_4, and evaporated under reduced pressure. The residue was purified by flash column chromatography (*n*-hexane–EtOAc as an eluent) and analyzed by chiral HPLC.

(*S*)-2-(4-Nitrophenoxy)propionic Acid (5b) obtained as result of KR of acyl chloride **2b** using amine (*S*)-**1a**. Yield 53 mg (83%), white solid, m.p. 87-89 °C. HPLC (Chiralcel OD-H, *n*-hexane-*i*PrOH-CF_3COOH 20:1:0.02): $\tau_{(R)\text{-}\mathbf{5b}}$ 23.4 min, $\tau_{(S)\text{-}\mathbf{5b}}$ 20.5 min; *ee* 88%. $[\alpha]_D$ = −41.2 (*c* = 1.0 in EtOH) (ref:[30] $[\alpha]_D$ = +48.7 (*c* = 1.0 in EtOH), (*R*)-**5b**, *ee* 98%). ^{1}H NMR (500 MHz, $CDCl_3$): δ = 7.89-8.54 (br. s, 1 H, COOH, overlapped with Ar signal), 8.21 (app. d, *J* = 9.2 Hz, 2 H, Ar), 6.95 (app. d, *J* = 9.2 Hz, 2 H, Ar), 4.91 (q, *J* = 6.9 Hz, 1 H, C^2H), 1.73 (d, *J* = 6.9 Hz, 3H, Me) ppm. ^{13}C NMR (125 MHz, $CDCl_3$): δ = 18.24, 72.21, 114.92, 125.99, 142.27, 162.09, 176.43 ppm. Anal. calcd. for $C_9H_9NO_5$: C, 51.19; H, 4.30; N, 6.63. Found: C, 51.05; H, 4.09; N, 6.82.

(*S*)-2-(4-Methoxyphenoxy)propionic Acid (5c) obtained as result of KR of acyl chloride **2c** using amine (*S*)-**1b**. Yield 51 mg (87%), yellowish oil. HPLC (Chiralpak AD, *n*-hexane–*i*PrOH–CF_3COOH 20:1:0.02): $\tau_{(S)\text{-}\mathbf{5c}}$ = 12.3 min, $\tau_{(R)\text{-}\mathbf{5c}}$ = 15.4 min; *ee* 71%. $[\alpha]_D$ = −29.4 (*c* = 0.54 in EtOH) (ref:[31] $[\alpha]_D$ = −42.7 (*c* = 0.95 in EtOH). ^{1}H NMR (400 MHz, $CDCl_3$): δ = 8.00-11.50 (br. s, 1 H, COOH), 6.86 (app. dt, *J* = 9.3, 2.7 Hz, 2 H, Ar), 6.82 (app. dt, 2 H, *J* = 9.3, 2.7 Hz, Ar), 4.70 (q, *J* = 6.9 Hz, 1 H, C^2H), 3.77 (s, 3 H, OMe), 1.63 (d, *J* = 6.9 Hz, 3 H, Me) ppm. ^{13}C NMR (125 MHz, $CDCl_3$): δ = 18.43, 55.64, 73.16, 114.75, 116.65, 151.23, 154.69, 177.93 ppm. HRMS (ESI): calcd. for $C_{10}H_{12}NaO_4^+$ $[M+Na]^+$ 219.0628; found 219.0624.

Acknowledgements

The work was financially supported by the Russian Science Foundation (grant 14-13-01077) in the part of kinetic resolution experiments and by the Ural Branch of the Russian Academy of Sciences (project AAAA-A18-118020290116-5) in the part of quantum chemical calculations. Analytical studies were carried out using equipment of the Centre for Joint Use "Spectroscopy and Analysis of Organic Compounds" at the Postovsky Institute of Organic Synthesis, Russian Academy of Sciences (Ural Branch). The quantum chemical calculations in the def2-TZVP basis set were performed using URAN Supercomputer at the Krasovskii Institute of Mathematics and Mechanics, Russian Academy of Sciences (Ural Branch), Ekaterinburg, Russia.

Keywords: acylation • kinetic resolution • diastereoselectivity • transition states • density functional calculations

[1] M. R. Maddani, J.-C. Fiaud, H. B. Kagan in *Separation of Enantiomers: Synthetic Methods* (Ed. M. Todd), Wiley-VCH, Weinheim, **2014**, pp. 13-74.

[2] a) E. Larionov, M. Mahesh, A. C. Spivey, W. Yin, H. J. Zipse, *J. Am. Chem. Soc.* **2012**, *134*, 9390-9399; b) L. Mesas-Sánchez, P. Dinér, *Chem. Eur. J*. **2015**, *21*, 5623-5631.

[3] a) X. Yang, V. D. Bumbu, P. Liu, X. Li, H. Jiang, E. W. Uffman, L. Guo, W. Zhang, X. Jiang, K. N. Houk, V. B. Birman, *J. Am. Chem. Soc*. **2012**, *134*, 17605-17612; b) Q. Peng, F. Duarte, R. S. Paton, *Chem. Soc. Rev*. **2016**, *45*, 6093-6107.

[4] V. P. Krasnov, D. A. Gruzdev, G. L. Levit, *Eur. J. Org. Chem*. **2012**, 1471-1493.

[5] a) D. A. Gruzdev, G. L. Levit, V. P. Krasnov, E. N. Chulakov, L. Sh. Sadretdinova, A. N. Grishakov, M. A. Ezhikova, M. I. Kodess, V. N. Charushin, *Tetrahedron: Asymmetry* **2010**, *21*, 936-942; b) D. A. Gruzdev, G. L. Levit, V. P. Krasnov, *Tetrahedron: Asymmetry* **2012**, *23*, 1640-1646; c) D. A. Gruzdev, S. A. Vakarov, G. L. Levit, V. P. Krasnov, *Chem. Heterocycl. Compd*. **2014**, *49*, 1795-1807.

[6] a) E. N. Chulakov, D. A. Gruzdev, G. L. Levit, L. Sh. Sadretdinova, V. P. Krasnov, V. N. Charushin, *Russ. Chem. Bull.* **2011**, *60*, 948-954; b) E. N. Chulakov, G. L. Levit, A. A. Tumashov, L. Sh. Sadretdinova, V. P. Krasnov, *Chem. Heterocycl. Compd*. **2012**, *48*, 724-732.

[7] a) S. A. Vakarov, D. A. Gruzdev, L. Sh. Sadretdinova, E. N. Chulakov, M. G. Pervova, M. A. Ezhikova, M. I. Kodess, G. L. Levit, V. P. Krasnov, *Tetrahedron: Asymmetry* **2015**, *26*, 312-319; b) S. A. Vakarov, D. A. Gruzdev, E. N. Chulakov, L. Sh. Sadretdinova, A. A. Tumashov, M. G. Pervova, M. A. Ezhikova, M. I. Kodess, G. L. Levit, V. P. Krasnov, V. N. Charushin, *Tetrahedron: Asymmetry* **2016**, *27*, 1231-1237.

[8] H. B. Kagan, J. C. Fiaud, *Top. Stereochem*. **1988**, *18*, 249-330.

[9] a) I. Hayakawa, T. Hiramitsu, Y. Tanaka, EP Patent 47005, 1982 (*Chem. Abstr.* **1982**, *97*, 55821b); b) V. N. Charushin, V. P. Krasnov, G. L. Levit, M. A. Korolyova, M. I. Kodess, O. N. Chupakhin, M. H. Kim, H. S. Lee, Y. J. Park, K.-C. Kim, *Tetrahedron*: *Asymmetry* **1999**, *10*, 2691-2702; c) P. A. Slepukhin, D. A. Gruzdev, E. N. Chulakov, G. L. Levit, V. P. Krasnov, V. N. Charushin, *Russ. Chem. Bull.* **2011**, *60*, 955-960.

[10] a) M. Hayashi, K. Wada, K. Munakata, *Agric. Biol. Chem.* **1983**, *47*, 2653-2655; b) P. Berlund, I. Vallikivi, L. Fransson, H. Dannacher, M. Holmquist, F. Björkling, O. Parve, K. Hult, *Tetrahedron: Asymmetry* **1999**, *10*, 4191-4202; c) R. S. Bezwada, US Patent 8901347, 2014 (*Chem. Abstr*. **2014**, *162*, 23018).

[11] a) J. Gabard, A. Collet, *Nouv J. Chim*. **1986**, *10*, 685-690; b) E. B. Rathbone, R. W. Butters, D. Cookson, J. L. Robinson, *J. Agric. Food Chem*. **1989**, *37*, 58-60; c) E. Boyd, S. Chavda, J. Eames, Y. Yohannes, *Tetrahedron: Asymmetry* **2007**, *18*, 476-482.

[12] a) R. J. E. Talbot in *Comprehensive Chemical Kinetics*, *Vol. 10* (Eds.: C. H. Bamford, C. F. H. Tipper), Elsevier, Amsterdam, **1972**, pp. 223-257; b) J. Keeler, P. Wothers, *Chemical Structure and Reactivity. An Integrated Approach*, Oxford University Press, Oxford, New York, **2008**, pp. 376-382.

[13] a) T. W. Bentley, G. E. Carter, H. C. Harris, *J. Chem. Soc., Perkin Trans*. **1985**, *2*, 983-990; b) A. Williams, *Acc. Chem. Res.* **1989**, *22*, 387–392; c) J. P. Guthrie, *J. Am. Chem. Soc*. **1991**, *113*, 3941–3949; d) T. W. Bentley, G. Llewellyn, J. A. McAlister, *J. Org. Chem*. **1996**, *61*, 7927–7932; e) A. C. Regan, C. I. F. Watt, *J. Phys. Org. Chem*. **2007**, *20*, 180-189.

[14] a) T. W. Bentley, *Int. J. Mol. Sci*. **2015**, *16*, 10601-10623; b) T. W. Bentley, H. Choi, H. Koo, D. N. Kevill, *J. Phys. Org. Chem*. **2017**, *30*, e3585.

[15] J. M. Fox, O. Dmitrenko, Lian-an-Liano, R. D. Bach, *J. Org. Chem.* **2004**, *69*, 7317-7328.

[16] a) S. E. Allen, S.-Y. Hsieh, O. Gutierrez, J. W. Bode, M. C. Kozlowski, *J. Am. Chem. Soc*. **2014**, *136*, 11783-11791; b) B. Wanner, I. Kreituss, O. Gutierrez, M. C. Kozlowski, J. W. Bode, *J. Am. Chem. Soc*. **2015**, *137*, 11491-11497.

[17] M. H. Hyun, J. S. Jin, J.-J. Ryoo, *Bull. Kor. Chem. Soc.* **1998**, *19*, 1393-1395.

[18] H. B. Bürgi, J. D. Dunitz, E. Shefter, *J. Am. Chem. Soc*. **1973**, *95*, 5065–5067.

[19] F. Ruff, Ö. Farkas, *J. Phys. Org. Chem.* **2010**, *24*, 480-491.

[20] E. H. Krenske, K. N. Houk, *Acc. Chem. Res*. **2013**, *46*, 979-989.

[21] D. Mikulski, K. Eder, M. Molski, *Comput. Theoret Chem.* **2014**, *1046*, 118-125.

[22] S. L. Capim, S. R. Santana, B. de Oliveira, G. B. Rocha, M. L. A. A. Vasconcellos, *J. Braz. Chem. Soc.* **2010**, *21*, 1718–1726.

[23] T. Sierański, *Struct. Chem*. **2016**, *27*, 1107–1120.

[24] A. Li, H. S. Muddana, M. K. Gilson, *J. Chem. Theory Comput*. **2014**, *10*, 1563-1575.

[25] L. Goerigk, S. Grimme, *Phys. Chem. Chem. Phys*. **2011**, *13*, 6670–6688.

[26] a) S. Grimme, S. Ehrlich, L. Goerigk, *J. Comput. Chem*. **2011**, *32*, 1456-1465; b) H. Kruse, L. Goerigk, S. Grimme, *J. Org. Chem.* **2012**, *77*, 10824-10834.

[27] a) L. Simon, J. M. Goodman, *Org. Biomol. Chem*. **2011**, *9*, 689-700; b) S. Grimme, A. Hansen, J. G. Brandenburg, C. Bannwarth, *Chem. Rev*. **2016**, *116*, 5105-5154.

[28] L. Goerigk, H. Kruse, S. Grimme, *Chem. Phys. Chem*. **2011**, *12*, 3421-3433.

[29] a) M. Chérest, H. Felkin, N. Prudent, *Tetrahedron Lett*. **1968**, *9*, 2199-2204; b) N. T. Anh, O. Eisenstein, *Tetrahedron Lett*. **1976**, *17*, 155-158; c) N. T. Anh, O. Eisenstein, *Nouv. J. Chim*. **1977**, *1*, 61-70; d) N. T. Anh, *Top. Curr. Chem*. **1980**, *88*, 145-182.

[30] J. Gabard, A. Collet, *Nouv. J. Chim.* **1986**, *10*, 685-690.

[31] E. B. Rathbone, R. W. Butters, D. Cookson, J. L. Robinson, *J. Agric. Food Chem.* **1989**, *37*, 58–60.

10.1002/ejoc.201800656